

A Real-Time Safety-Based Optimal Velocity Model

AWAD ABDELHALIM^{1b} AND MONTASIR ABBAS^{1b} (Member, IEEE)

The Charles Edward Via, Jr. Department of Civil and Environmental Engineering, Virginia Polytechnic Institute and State University (Virginia Tech), Blacksburg, VA 24061, USA

CORRESPONDING AUTHOR: M. ABBAS (e-mail: abbas@vt.edu)

This work was supported by the Virginia Tech's Open Access Subvention Fund.

ABSTRACT Modeling safety-critical driver behavior at signalized intersections needs to account for the driver's planned decision process, where a driver executes a plan to avoid collision in multiple time steps. Such a process can be embedded in the Optimal Velocity Model (OVM) that traditionally assumes that drivers base their "mental intention" on a distance gap only. We propose and evaluate a data-driven OVM based on real-time inference of roadside traffic video data. First, we extract vehicle trajectory data from roadside traffic footage through our advanced video processing algorithm (VT-Lane) for a study site in Blacksburg, VA, USA. Vehicles engaged in car-following episodes are then identified within the extracted vehicle trajectories database, and the real-time time-to-collision (TTC) is calculated for all car-following instances. Then, we analyze the driver behavior to predict the shape of the underlying TTC-based desired velocity function. A clustering approach is used to assess car-following behavior heterogeneity and understand the reasons behind outlying driving behaviors at the intersection to design our model accordingly. The results of this assessment show that the calibrated TTC-based OVM can replicate the observed driving behavior by capturing the acceleration pattern with an error 20% lower than the gap distance-based OVM.

INDEX TERMS Driver behavior calibration, intersection safety, optimal velocity model, vehicle trajectory tracking.

I. INTRODUCTION

VEHICLE trajectory tracking is one of the major areas of research in Intelligent Transportation Systems (ITS), and is integral to other ITS applications that include driver behavior and car-following analysis, dynamic signal timing, active traffic management, advanced driver-assistance systems (ADAS), among others. The combination of trajectory tracking and driver behavior analysis is key in identifying risks and conflicts that may lead to crashes, allowing practitioners to proactively implement mitigation measures. Both the tasks of accurate and efficient vehicle trajectory tracking and driving behavior modeling remain challenging. Most car-following models (e.g., Gazis-Herman-Rothery (GHR), Wiedemann, Fritzsche) assume that drivers make longitudinal decisions (i.e., acceleration) based on assumed momentary stimuli inputs. For example, the GHR model [1] predicts a driver's acceleration based on the current driver's speed and the sensed difference in speed

and distance from the leading vehicle. These models do not account for the driver's planned decision process, where a driver could perceive an impending danger, and plans to avoid that danger, then executes that plan in multiple time steps. This is especially important when modeling safety-critical or close-to-critical situations, when an ego vehicle approaches a vehicle that slows down, forcing the driver of the ego vehicle to start a process of avoidance or adjustment in their speed trajectory.

There is, therefore, a need to estimate the driver intention underlying policy. This policy is expected to potentially vary among drivers (causing heterogeneity in driver behavior). It might also change for the same driver based on the driving context (e.g., driving on a freeway versus driving on an arterial, executing a turning movement versus continuing straight through an intersection, etc.). Therefore, the policy can take a variable functional form that maps the perceived state into an action plan (a series of maneuvers or a deceleration profile). The closest form of an existing implementation of such an approach can be found in models that attempt to capture a latent driving intention function and then translates that

The review of this article was arranged by Associate Editor Emmanouil Chaniotakis.

into a predicted desired acceleration. The Optimal Velocity Model (OVM) [2] is an example of such an approach, albeit not explicitly designed with the safety-related input in mind. Instead, the OVM uses the difference in distance between the following and leading vehicle to estimate a desired optimal velocity (using a hyperbolic tangent function form), then uses the difference between that estimated velocity and current velocity, as well as an intended time-to-execution parameter, to come up with the desired acceleration/deceleration. The issue with the OVM (in this context) is that it assumes that drivers base their “mental intention” on a difference in the distance only. Whereas in safety-critical situations, drivers are more likely to change their intention based on their estimate of the impending danger, as could be measured, for example, by the time-to-collision parameter (TTC).

A. OBJECTIVE

This paper examines the hypothesis that using a car-following model based on real-time TTC can better capture the actual driver behavior at urban intersections. We present a case study for a site in Blacksburg, VA, USA. Vehicle trajectories are extracted from a roadside video footage. Vehicles engaging in car-following episodes are then identified and an iterative optimization process is formulated to calibrate the parameters of the Optimal Velocity Model (OVM) in terms of the estimated instantaneous time-to-collision. The following sections of this paper are as follows: (II) a survey of related literature in driver behavior modeling, vehicle tracking, and trajectory-based safety, (III) a detailed breakdown of trajectory data extraction and safety-based model calibration, (IV) results and analyses of the case study, and, (V) discussion and conclusions.

II. RELATED WORK

A. CAR-FOLLOWING BEHAVIOR MODELING

Car-following and driver behavior modeling has long been one of the most well studied topics in traffic engineering. Brackstone and McDonald [3] provided a systemic reexamination of the then-existing car-following models, including the GHR model, collision avoidance, linear, fuzzy logic-based and psycho-physical models. They concluded that albeit the extensive study of car-following models, and the strong support of those models in terms of conceptual bases and empirical data, the lack of time-series following behavior is a significant limitation to those models. The emergence of naturalistic driving and trajectory datasets and algorithms [4] alongside advancements in traffic simulation modeling provided a boost to the state-of-the-research allowing researchers to assess driving behavior and car-following under different traffic conditions, driver attention and distraction scenarios, and in various roadway geometry settings [5], [6], [7], [8], [9], [10].

One of the most widely adopted driver behavior models is the Optimal Velocity Model proposed by Bando *et al.* [2]. The base model developed by Bando *et al.* was very successful in describing traffic and capturing behavior during

congestion, inspiring the development of OVM-derived models to help capture further aspects of traffic flow more realistically. Wang *et al.* [11] proposed an OVM variation with a modified optimal velocity function. Mammari *et al.* [12] investigated whether a modified OVM using the inverse of TTC as a weighing factor at given distance gap increments would better capture the breaking state of following vehicles. The proposed model was only tested hypothetically in simulation, finding that the simulated drivers’ risk perception of rear-end collision could be significantly improved. Lazar *et al.* expanded on this work [13] and also provided an exhaustive review of some of those models [14] concluding that due to the high variability in driving behavior, each model performs well under certain circumstances and has evident weaknesses in other circumstances. There is, therefore, a need and an immense value in developing data-driven models that would take into account the observed driver behavior heterogeneity [15], and in case of urban intersections, factors such as turn movement classification and signal timing, which all impact the drivers’ decision making processes during car-following episodes. The recent advancements in the fields of vehicle tracking and the growing availability of trajectory data and trajectory-extraction methods make the creation of such data-driven models achievable and necessary.

This newfound availability of trajectory data in recent years has enabled researchers to move from the long-standing models to developing driver behavior models that utilize modern machine learning methods, with a focus on neural and Bayesian networks [16], [17]. Those data-driven models have proven to produce substantial improvements, and overcome the limitations of the conventional, mathematically derived models, especially the tedious process of parameter calibration [18], [19]. Traditional models, however, are based on traffic flow theory fundamentals and hence are highly explainable. The current incomprehensible nature of black-box data-driven models is a major drawback in that regard. Another limitation in the existing literature is the dependence of assessment on long-standing datasets extracted at certain locations from video inference [20] and instrumented vehicles [21] that require further assessment on their transferability to other locations where driver behavior may significantly vary. The evolving automotive technologies over the years may also impact driver behavior in the same location (improved vehicle performance and dynamics, on-board ADAS, etc), hence there is a need for a more robust and generalizable approach utilizing advances in real-time trajectory extraction.

B. VEHICLE DETECTION AND TRACKING FOR TRAFFIC SAFETY

This growing ability to extract and analyze high-quality trajectory data has also enabled researchers to move from developing predictive crash likelihood models based on historical data to a more proactive approach of real-time assessment of traffic safety surrogate measures [22], [23].

Those studies assessed different safety surrogate measures, but the time to collision is the most commonly used measure. St-Aubin *et al.* have proposed a video inference based safety surrogate framework and thoroughly assessed it in multiple studies [24], [25], [26]. Xie *et al.* [27], [28] developed a framework to comprehensively assess traffic safety from video data by analyzing conflict risk and TTC on hourly basis, and found a significant correlation between the actual number of crashes and the traffic conflicts inferred through their proposed framework. Das and Maurya [29] utilized trajectory data extracted from an urban traffic environment to assess traffic safety based on the interactions of TTC, roadway center line separation, and leader-follower vehicle type pairing. Estimating TTC from video data is an ongoing research problem, recent studies have assessed TTC estimation from on-board [30] and UAV [31] cameras.

Recent studies both in the fields of traffic safety and driving behavior modeling show the promising prospects of utilizing trajectory data obtained from video inference and conducting TTC-based safety assessments. A recent review study by Li *et al.* [32] concluded that there is a need and immense potential in data-driven, trajectory-based driver behavior modeling. Therefore, this paper aims to address the gaps identified in the literature, both in terms of the OVM's formulation and data acquisition for the model's calibration, by proposing and assessing a data-driven car-following behavior model that can utilize the real-time high-resolution safety assessment, in terms of instantaneous TTC, obtained from roadside video inference.

III. METHODOLOGY

A. PREVIOUS WORK

In previous works we proposed and evaluated VT-Lane, a computer vision-based framework real-time vehicle tracking and detection. We implemented a combination of YOLO v4 [33] and DeepSORT [34] algorithms for the tasks of vehicle detection and trajectory tracking, respectively. We then introduced the concept of NEMA phases-based virtual traffic lanes to obtain vehicle turn movement counts and address issues of vehicle identity switching which results from occlusion. The base of the framework is detailed and evaluated in [35] and [36]. The method used for reference object scaling, distance and speed estimation is discussed and assessed in detail in [37]. A flowchart showing the extended end-to-end framework utilized in this study is shown in Figure 1.

B. VEHICLE TRACKING, MOVEMENT CLASSIFICATION, AND SPEED ESTIMATION FRAMEWORK

For this study, we utilize an extended VT-Lane framework for the task of vehicle tracking and turn movement classification. To improve the accuracy of vehicle tracking in congested traffic, we retrained the Deep-SORT tracker on the UA-Detrac dataset [38], a benchmark dataset for multi-object detection and tracking consisting of 10 hours of

video data with over 1.2 million bounding boxes of traffic-related objects. Retraining the tracker on different vehicle movements, types, occlusion factors, and glare conditions as illustrated in Figure 2 and incorporating low-confidence track filtering [39] resulted in significant performance improvements in congested traffic conditions. In the United States, the typical traffic pattern assignment for signal controllers follows the National Electrical Manufacturers Association (NEMA) standards shown in Fig. 3 [40]. Figure 4 shows the site of this study from the perspective of the roadside camera used to obtain the video data for this study. The figure also illustrates the NEMA movement enumeration for the site.

C. TIME TO COLLISION ESTIMATION

Following trajectory extraction and speed estimation, the time to collision is calculated for all vehicle pairs broken down by their virtual NEMA movement lane. For the study intersection shown in Figure 4, NEMA movements 2 and 6 have two lanes, resulting in 10 virtual lanes across the intersection (right turners included with through moving vehicles). The classification of vehicle movements via our framework eases the task of calculating the time to collision, as it inherently identifies vehicles that are moving in the same lane regardless of their location inside the intersection's geometry. The length of vehicles reported in the output database is used to calculate effective bumper-to-bumper distance as illustrated in Figure 5, which is used to calculate the time to collision as shown in Equation (1) for the following vehicle based on the speed differential for every pair of vehicles detected moving in the same virtual lane within the same frame.

$$TTC_{i,n,k} = \frac{\Delta \text{Distance} - \frac{1}{2}(L_{i,n,k} + L_{i-1,n,k}) * \gamma}{\Delta \text{Speed}} \forall_{i,n,k} \quad (1)$$

where:

$TTC_{i,n,k}$ = Time to collision in *seconds* for vehicle i to the leading vehicle $i-1$ moving in the same NEMA virtual lane n during frame k .

$\Delta \text{Distance}$ = The Euclidean distance between the centroids of detection boxes of the leading and following vehicle.

$L_{i,n,k}$ = Length of vehicle i during frame k in *pixels* (vehicle length changes slightly as it traverses the intersection due to the vanishing point problem).

γ = Conversion function for vehicle length in *pixels* to *meters* incorporating a pixel-per-meter weight function.

ΔSpeed = The speed differential between the following and leading vehicles (i.e., $\text{Speed}_{i,n,k} - \text{Speed}_{i-1,n,k}$) in *meter/sec*.

A negative speed differential occurs when the leading is moving faster than the following vehicle, resulting in a negative TTC meaning that the vehicles will not collide.

To calculate the real-time TTC, during every frame of the input video, vehicles engaged in car-following episodes are surveyed within each virtual traffic lane. If a car-following episode exists within a virtual lane, and the speed differential is positive (i.e., the following vehicle is closing the gap to

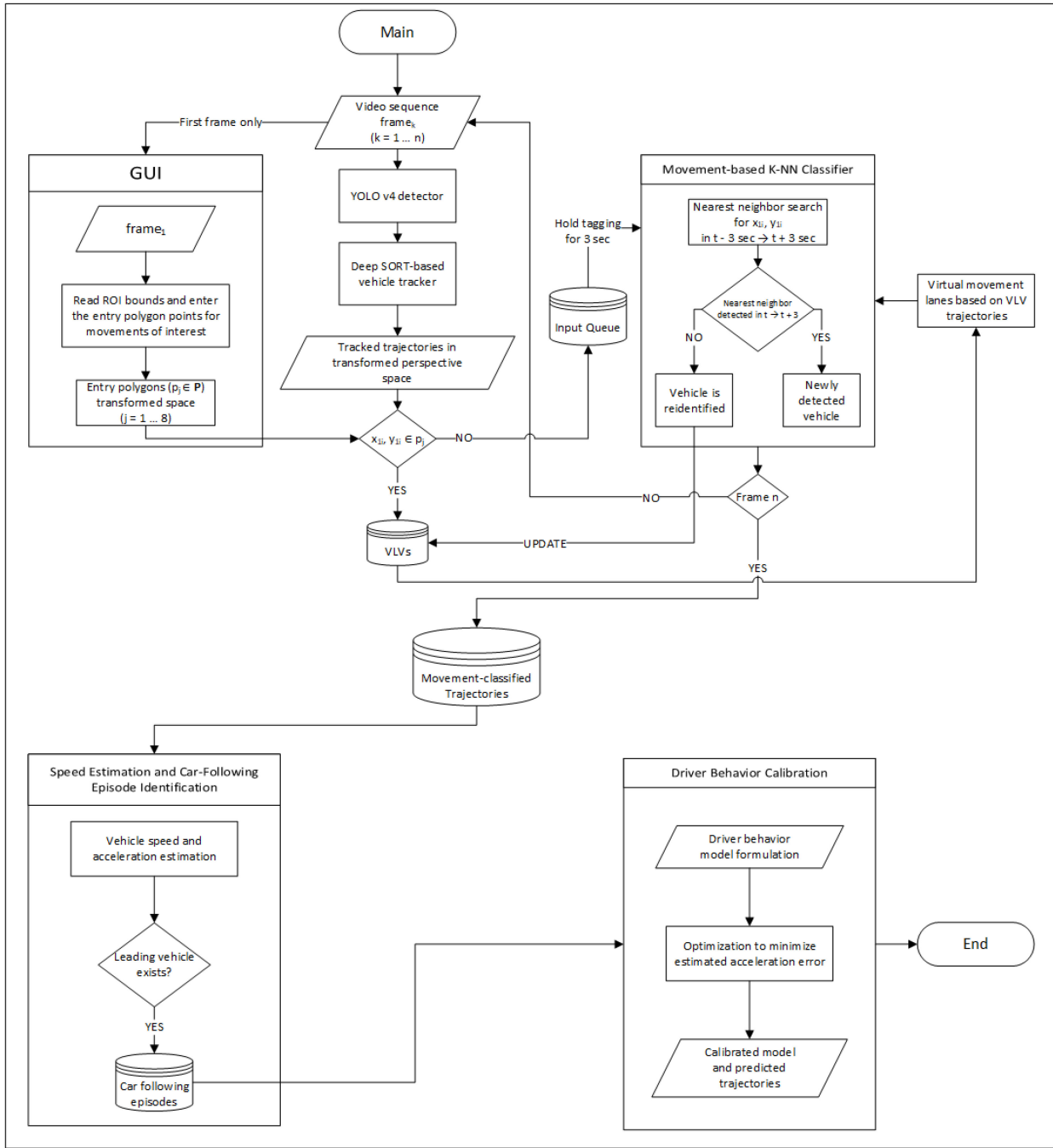


FIGURE 1. VT-Lane framework's data flow and trajectory data utilization for real-time driving behavior modeling.

the leading vehicle) the TTC is calculated. Otherwise, the TTC is assigned a value of infinity for that instance of the car-following episode. This process is shown in Algorithm 1.

D. TTC-BASED OPTIMAL VELOCITY MODEL CALIBRATION

Following TTC calculation, vehicles engaging in car-following episodes are identified based on the threshold shown in Equation (2). This assumes that a following driver's behavior is not influenced by the leading vehicle if the

estimated instantaneous TTC is greater than 20 seconds.

$$\text{Leading Vehicle} = \begin{cases} \text{vehicle}_{i-1, n}, & \text{if } \text{TTC} \leq 20\text{s} \\ \text{None}, & \text{otherwise} \end{cases} \quad (2)$$

We then assess the value of utilizing the instantaneous TTC estimates for calibrating car-following models. For the purpose of exploratory assessment in this study, we utilize the base Optimal Velocity Model. The optimal velocity of a following vehicle based on the distance gap is given by Equation (3), from which the desired acceleration is

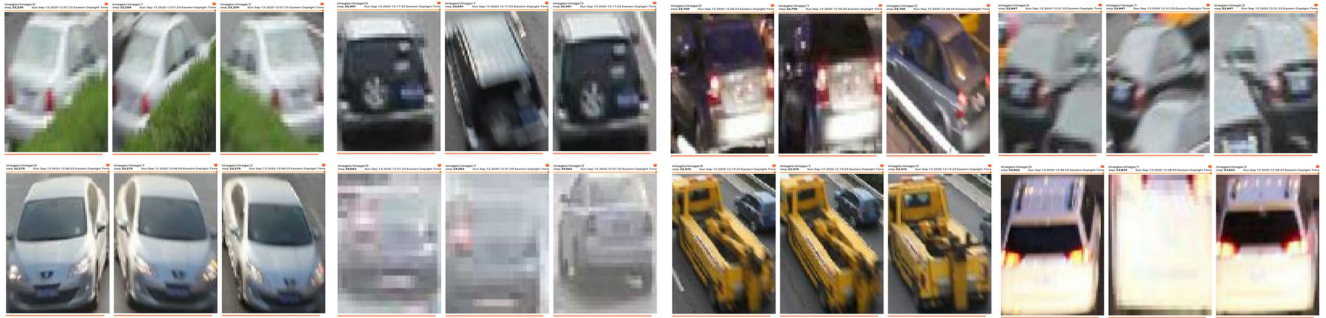


FIGURE 2. Tracker retraining on the UA-Detrac dataset.

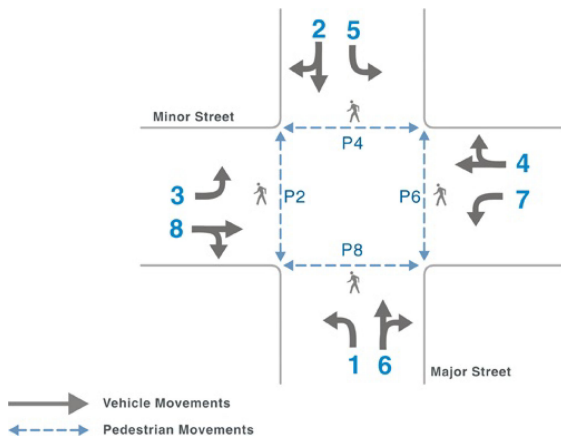


FIGURE 3. Typical 8-phase traffic controller operation [40].

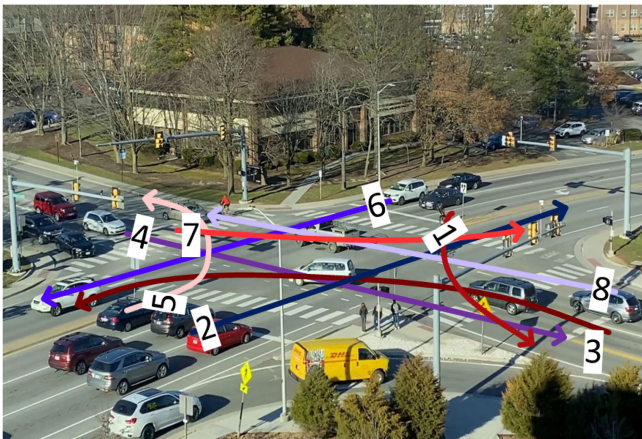


FIGURE 4. Site of study and NEMA movements.

calculated using Equation (4).

$$v_{opt}(s) = v_o \frac{\tanh\left(\frac{s}{\Delta s} - \beta\right) + \tanh \beta}{1 + \tanh \beta} \quad (3)$$

$$\dot{v} = \frac{v_{opt}(s) - v}{\tau} \quad (4)$$

where:

s = Distance gap between vehicles in a car-following episode (m).

$v_{opt}(s)$ = The theoretical optimal velocity for a given distance gap (km/hr).

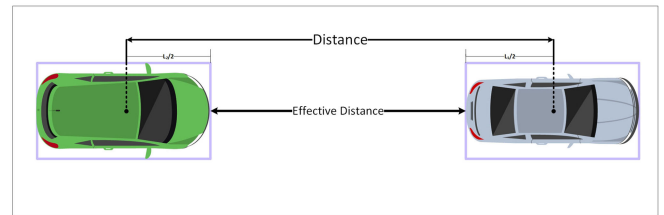


FIGURE 5. Effective bumper-to-bumper distance for time to collision calculation.

Algorithm 1: Time to Collision Calculation

Result: Calculating TTC for Vehicle Pairs Crossing the Intersection

initialization;

for $frame_k$ **do**

for $virtual_lane_n$ **do**

if $COUNT(car_n) < 2$ **then**

 Continue;

else

if $car_i \exists car_{i-1} \ \& \iff \Delta Speed \in \mathbb{R}^+$

then

 Calculate $TTC_{i,n,k}$;

else

$TTC_{i,n,k} \leftarrow \infty$

end

end

end

end

v_o = Desired speed (km/hr), Δs = Transition width (m).

β = Form Factor, \dot{v} = OVM acceleration ($km/hr/sec$).

v = Actual speed of a following vehicle (km/hr).

τ = Adaptation time (sec).

Alongside calibrating the model in terms of the distance gap between vehicle pairs, we calibrate in terms of the estimated real-time TTC. We also introduce a data-driven modified acceleration function (MAF) capturing the observed car-following behavior from video inference.

$$v_{opt}(ttc) = v_o \frac{\tanh\left(\frac{ttc}{\Delta s_{ttc}} - \beta\right) + \tanh \beta}{1 + \tanh \beta} \quad (5)$$

Algorithm 2: OVM Parameter Calibration

Result: Calibrating the parameters of OVM in terms of estimated TTC.

initialization;

for movement_{*i*} ∈ {through, turning} **do**

for episode_{*j*} **do**

for instance_{*k*} **do**

$$v_{opt_{j,k}} \leftarrow v_o \frac{\tanh\left(\frac{ttc}{\Delta s_{ttc}} - \beta\right) + \tanh \beta}{1 + \tanh \beta};$$

$$\dot{v}_{j,k} \leftarrow (1 - \alpha) \frac{v_{opt_{j,k}} - v_{j,k}}{\tau} + \alpha f(ttc_{observed});$$

$$error_{j,k} \leftarrow (a_{j,k} - \dot{v}_{j,k})^2;$$

end

end

$$MSE_i \leftarrow \frac{1}{n_{instances_i}} \sum_{j=1}^{n_{episodes_i}} \sum_{k=1}^{n_{instances_j}} error_{j,k}$$

end

$$\dot{v} = (1 - \alpha) \frac{v_{opt}(ttc_{instance}) - v}{\tau} + \alpha f(ttc_{observed}) \quad (6)$$

where α is a weight parameter assigned to the observed ttc-based function that is learned from the extracted trajectory data, $f(ttc_{observed})$. Furthermore, we utilize the turn movement classification from VT-Lane to produce separate calibrated models for through moving vehicles and turning vehicles for the intersection of study as described in Algorithm 2. For the following vehicle in each episode_{*j*} of movement type_{*i*} (where *i* is either through or turning movement), the OVM acceleration \dot{v} during instance_{*k*} of the episode is calculated based on the estimated TTC between the leading and following vehicles. The true instantaneous acceleration (*a*) of vehicles is calculated based on their frame to frame speed changes. An optimization problem is formulated to minimize the Mean Square Error of the true acceleration vs OVM acceleration by calibrating the parameters of the OVM model (v_o , Δs , β , τ , and α).

IV. RESULTS AND ANALYSIS

A. VIDEO INFERENCE AND VEHICLE TRAJECTORY EXTRACTION

A 1-hour footage was recorded and analyzed for the study intersection during the PM peak hour. The trajectory extraction and movement classification obtained via VT-Lane is illustrated in Figure 6. A total of 2,656 vehicles were detected and tracked for the full 1-hr footage. Table 1 shows a sample of the actual and detected counts from a 30-minute video segment.

Alongside the vehicle trajectories and movement classification, car-following episodes were identified, the instantaneous speed and distance differentials were estimated, and the time to collision was calculated accordingly. A total of 588 car-following episodes were identified for the 1-hr video data. Figure 7 shows a sample car-following episode. For both the acceleration and TTC calculations, a Savitzky–Golay filter was applied to obtain smoother estimates.

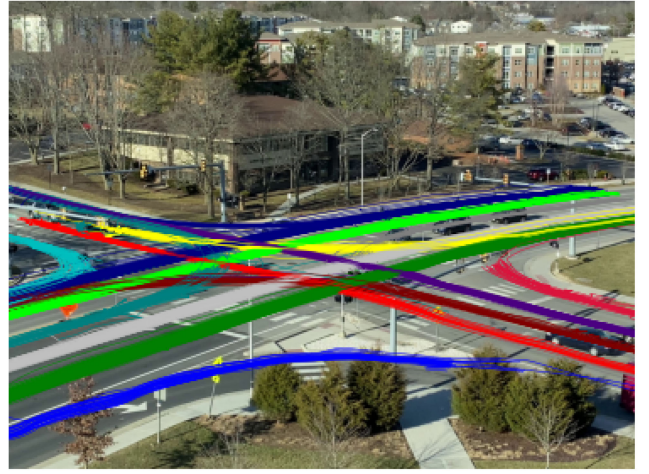


FIGURE 6. Trajectories and turn movement classification.

TABLE 1. 30-minute actual vs detected turn counts.

NEMA Phase	Actual	Detected	Accuracy (%)
2	438	415	95
5	69	62	90
4	93	81	87
7	53	49	92
6	421	398	94
1	31	30	97
8	52	47	90
3	137	129	94
Total	1294	1211	93.5%

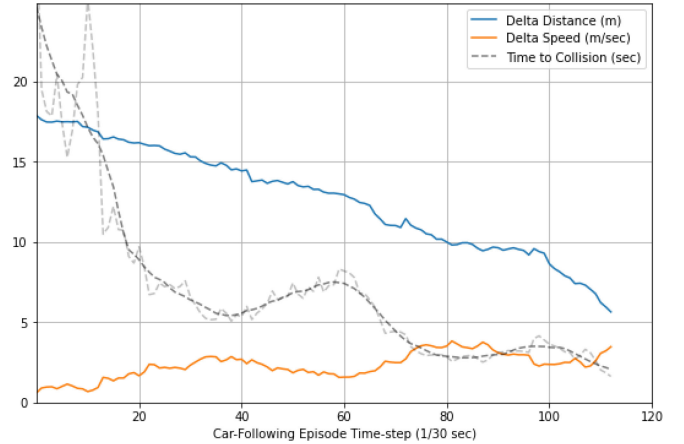
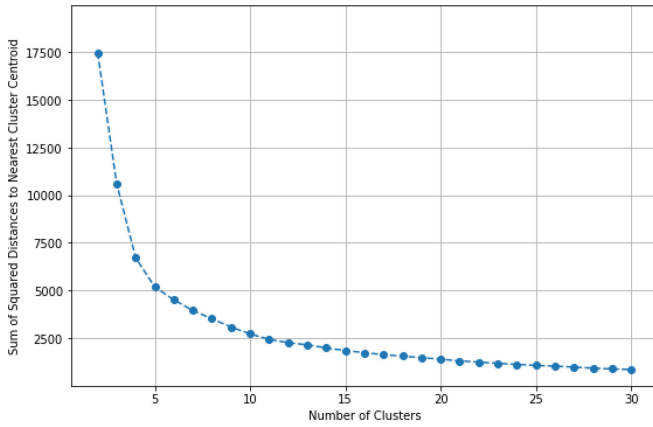


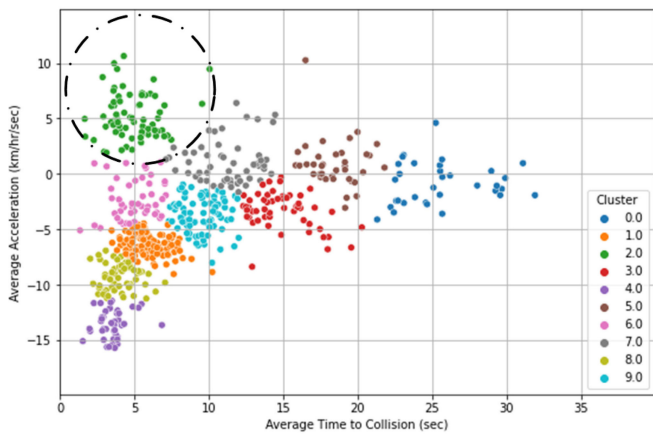
FIGURE 7. Sample car-following episode.

B. MODEL CALIBRATION

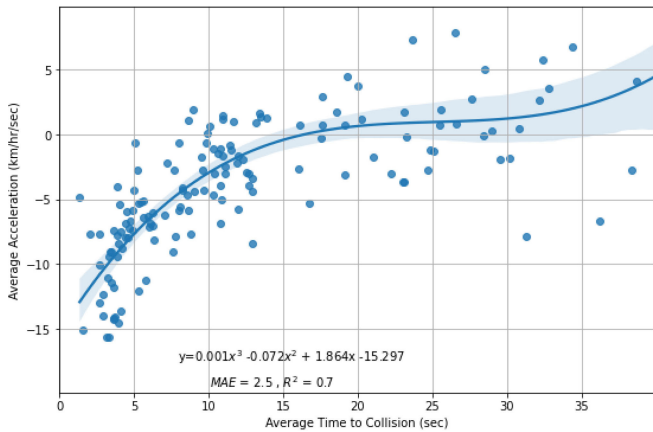
Prior to model calibration, we plot the average acceleration versus time to collision for all 588 car-following episodes. This was carried out to identify outlying behavior that would bias the model. A threshold of ten clusters emerged as one after which no significant reduction in distance to nearest centroid was achieved to justify further clustering as illustrated in Figure 8 a. When grouping the episodes into ten



(a) Total error vs number of driving behavior clusters.



(b) Identifying outlying driving behavior cluster.



(c) Data-driven deceleration function from observed behavior.

FIGURE 8. Behavior clustering and data-driven function fit.

clusters, an outlying behavior cluster was identified (shown in Figure 8 b) where following vehicles seemed to be accelerating despite the lower TTC (≤ 5 seconds). All members of this cluster (72 episodes) were found to be episodes belonging to NEMA phase 6, which, alongside phase 2 had the highest volumes. One of the two lanes of phase 6, however, was a shared lane with right turners, resulting in higher

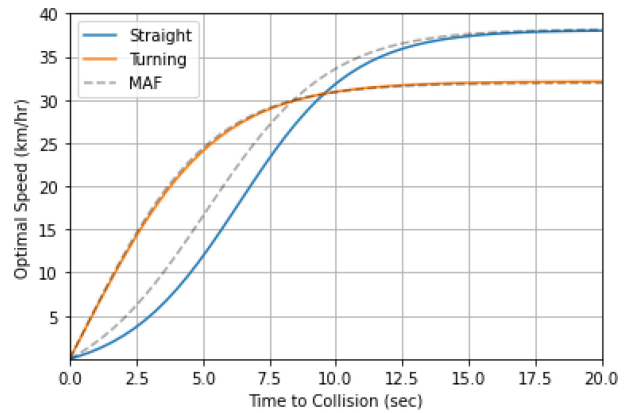


FIGURE 9. Real-time TTC-based optimal velocity function.

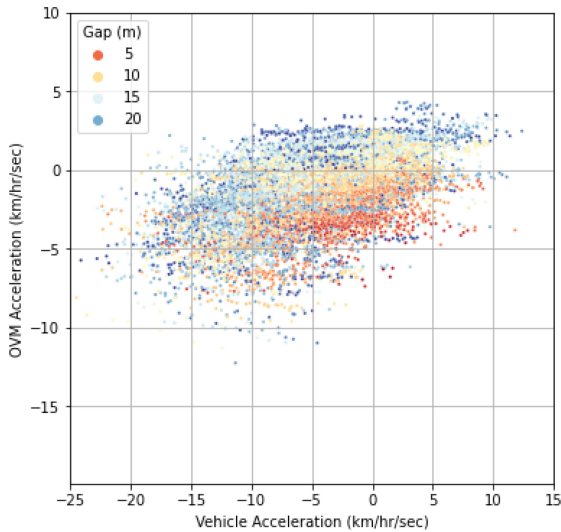
TABLE 2. Optimal parameters for the calibrated models.

	Base OVM	Base OVM		TTC-Based		TTC-MAF	
		Thu	Trn	Thu	Trn	Thu	Trn
Δs	9.41	9.98	4.09	4.28	4.93	4.63	4.76
β	0.10	0.10	0.13	1.48	0.11	1.10	0.10
τ	5.12	4.37	4.20	6.49	5.89	6.11	5.83
v_o	36.13	39.63	31.04	38.07	32.13	38.20	31.95
α	-	-	-	-	-	0.18	0.01

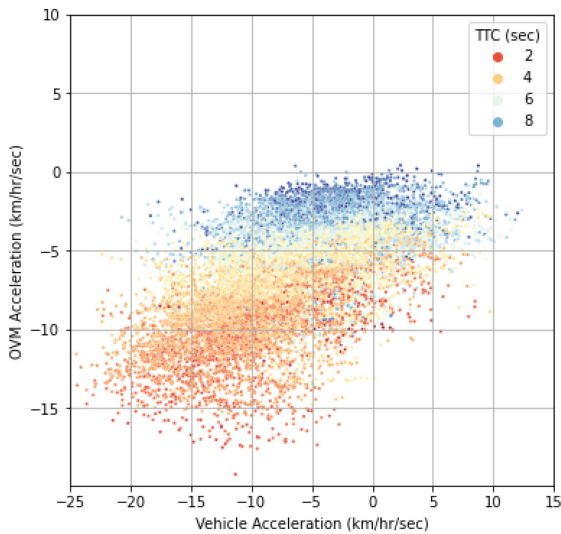
queues, and hence the acceleration behavior was significantly higher for episodes in this phase compared to the remaining NEMA movements.

After identifying the outlying behavior and understanding its causes, we took a 20% subset of the remaining observed episodes (516 episodes) to fit a function that captures the observed deceleration behavior based on TTC. The function is added with a weighing factor (α) to the OVM's acceleration function. A 3rd order polynomial was found enough to capture the observed behavior to a satisfactory extent, with a mean absolute error of 2.5 km/hr/sec and an R^2 of 0.70. Figure 9 shows the optimal speed function of the calibrated OVM as a function of the TTC (the dotted line shows the TTC-Based model with modified acceleration function, which can be seen providing less conservative optimal velocities).

Table 2 shows the optimal model parameters for the base, the TTC-Based OVM, and the model employing the modified acceleration function (MAF) denoted TTC-MAF. The parameters of the Base OVM were optimized based on the gap distance for all episodes, then employing the movement classification obtained from VT-Lane. Intuitively, both the base and TTC-Based models were optimal with a lower desired speed threshold for turning movements compared to through movements. It should be noted that the Δs parameter is in meters for the base model, and in seconds for the TTC-Based model. The adaptation time τ is in frames (given that the input is in instantaneous, frame-based data), which translates to 0.20-0.25 seconds. This relatively short



(a) Gap-Based OVM.



(b) TTC-Based OVM.

FIGURE 10. Sample episodes from video inference.

adaptation time is attributed to the intersection nature of the area of the study where drivers make quick decisions. The desired velocities (v_o) are in km/hr, and variables β and α are unitless.

Given that the OVM doesn't explicitly account for vehicle dynamics, this less conservative optimal velocity function due to the proposed modification based on observed behavior may lead to improved performance in microscopic simulation. The α parameter (weight assigned to the observed acceleration function in the modified TTC-Based model) was close to zero for turning movements. This is attributed to the fact that turning movement car-following episodes only accounted for 7% of all episodes identified, hence the function from the observed 20% subset was more representative of through moving vehicles.

Figure 10 shows the actual vs OVM calculated acceleration for all instances of car-following episodes. The figure

TABLE 3. Instantaneous acceleration error (km/hr/sec).

	Base OVM	Base OVM		TTC-Based		TTC-MAF	
		Thu	Trn	Thu	Trn	Thu	Trn
MSE	4.30	4.33	3.80	3.49	3.55	3.45	3.55
mean	-0.01	-0.02	0.09	-0.18	-0.05	-0.10	-0.09
σ	5.46	5.49	4.95	4.42	4.63	4.39	4.63
5%	-8.37	-8.29	-8.15	-7.04	-7.57	-6.92	-7.55
25%	-3.68	-3.79	-2.89	-3.14	-2.98	-3.03	-2.99
50%	-0.33	-0.43	0.07	-0.37	-0.01	-0.31	-0.02
75%	3.44	3.42	2.91	2.56	2.62	2.62	2.61
90%	7.13	7.21	6.38	5.60	5.42	5.61	5.43
95%	9.50	9.63	8.68	7.53	7.75	7.50	7.76

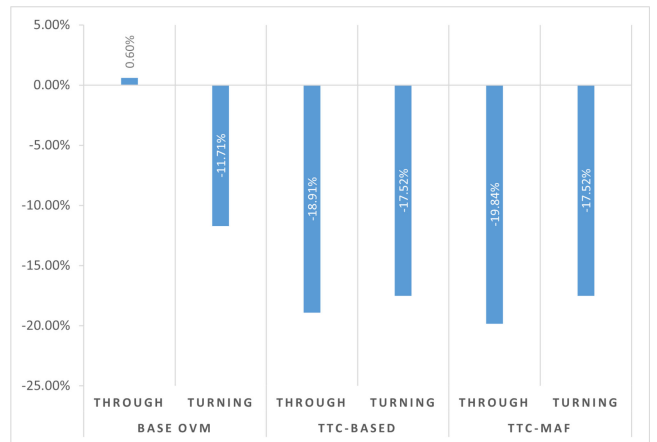


FIGURE 11. Percentage of change in error compared to base OVM.

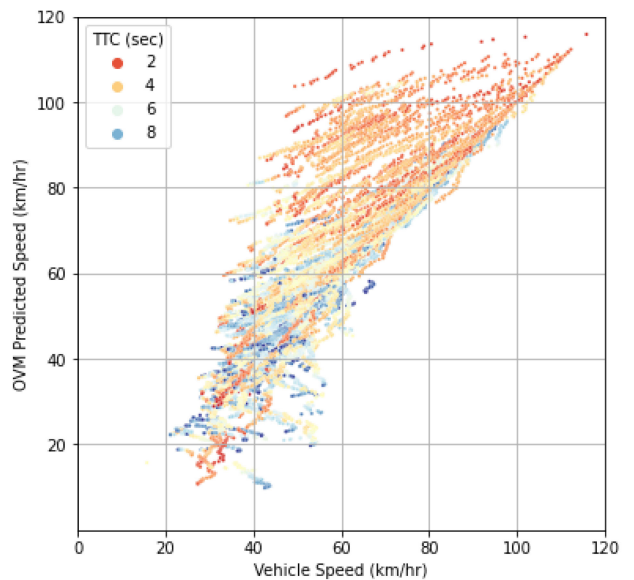


FIGURE 12. Actual vs TTC-based model predicted speeds.

clearly illustrates that the TTC-Based model provides better prediction of the deceleration behavior and can be much better interpreted. Figure 10 (a) for the original gap-based OVM

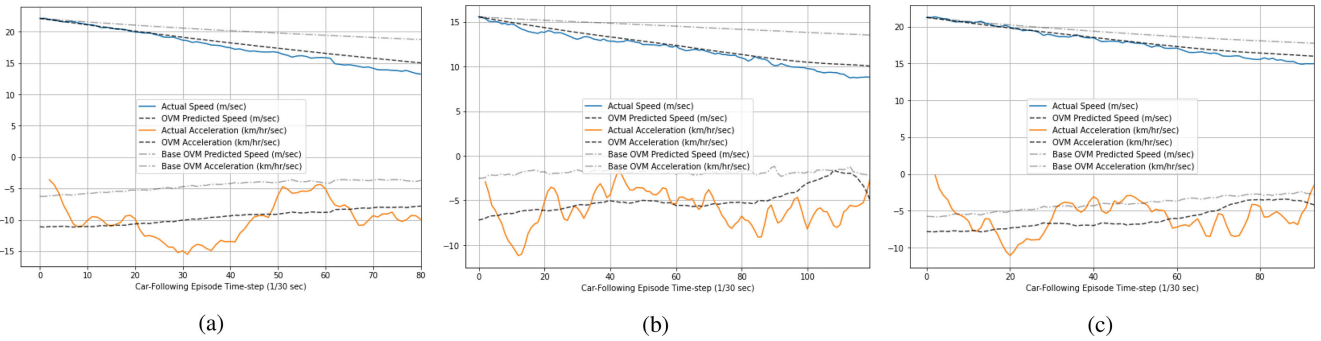


FIGURE 13. Sample episodes and model predicted speed and acceleration profiles.

is color-coded with the distance gap (0-20+ m) whereas Figure 10 (b) for our TTC-based model is color-coded with the TTC (0-10+ seconds). While no clear association can be identified in Figure 10 (a), the association between the following vehicles' acceleration and TTC is very clear in the TTC-Based model, where vehicles are accelerating or maintaining speed at higher TTC estimates, and decelerating as TTC decreases. It can be observed that the TTC-Based model provides a significantly better prediction of deceleration process.

It can also be observed in Table 3 that the TTC-Based model results in significant improvements in the MSE and standard deviation of errors compared to the base distance-based model. Improvements were slightly lower for turning movements. This is attributed to the fact that only 43 of the 588 episodes identified were turning, hence the availability of more data for through movements resulted in a better calibrated model. The percentage of change in error compared to the base OVM model (distance-based model without accounting for turning movement classification from video inference) is illustrated in Figure 11.

The figure illustrates that introducing turning movement classification alone leads to significant improvement in the base model's performance for capturing the car-following behavior of vehicles executing turning movements. Substantial improvements are achieved via the TTC-Based model, with the TTC-Based MAF model having an error 19.84% lower than the base model.

Figure 12 shows a plot of the actual versus TTC-Based model predicted speeds (color-coded with the TTC) for all instances of car-following inferred from the 1-hr footage. Intuitively, lower TTCs were associated with following vehicles driving at high speeds, and vice-versa. The plot also illustrates that the model performed significantly better at lower following speeds, while the variance increased at speeds higher than 50 km/hr. The average error in instantaneous speeds estimation was found to be 4.74 km/hr for through movements, and 0.54 km/hr for turning movements.

Finally, Figure 13 shows sample episodes, illustrating the actual speed and acceleration profiles of the following vehicles, the calibrated TTC-MAF OVM acceleration, and the

resulting speed profile. The calibrated model captures the acceleration/deceleration behavior well enough to produce comparable speed profiles to the actual data, despite the instability of acceleration estimation induced by the high-resolution of video inference (at 28-30 fps). The results not only illustrate the accuracy with which the calibrated model is able to capture the actual deceleration pattern, but also the high stability at which this is accomplished (i.e., no severe abrupt acceleration or deceleration). The figure also shows the predicted acceleration and speed profile obtained using the calibrated distance-based model (Base OVM), showcasing the improvement obtained via our model.

V. DISCUSSION AND CONCLUSION

In this study, we examined and assessed the value of driver behavior modeling based on real-time vehicle trajectories and time-to-collision inferred from traffic video data. We utilized the ability of our VT-Lane framework to efficiently extract accurate vehicle trajectories, movement classification, and speed estimates to calibrate the parameters of the Optimal Velocity Model for the area of study both in terms of the distance gap and the estimated TTC from video inference. The TTC-Based model was able to produce improved deceleration estimates for vehicles engaged in car-following episodes, and result in speed profiles with an instantaneous estimated speed error of 4.74 km/hr and an instantaneous acceleration error 19.84% lower than that of the base, distance-based model. The results obtained utilizing real-time data and through the modified acceleration function based on observed behavior show the high value of infusing driving behavior models with data-driven modifications.

The clear differences in model parameters between straight moving vehicles and vehicles executing turning movements at the intersection demonstrates the need for taking into account such characteristics in modeling driving behavior at urban settings. While 3rd order polynomial function was able to capture the observed driving behavior with high reliability (R^2 of 70%), further information that can be obtained through video inference (including, and not limited to signal status time, vehicle type,

overall traffic density and lane occupancy, etc) can all be utilized to develop more sophisticated observed driving behavior functions that would potentially further improve the performance the data-driven model. Given the high-resolution and accuracy of the trajectories obtained through VT-Lane, utilizing a Kalman filter or similar continuous state estimation approach to improve the desired acceleration estimates based on the continuity of the trajectory instead of relying on single measurements is another route worth exploring.

The short length of the car-following episodes, given that vehicles are only tracked as they cross the intersection, was a limiting factor for this study. Although vehicles engaged in car-following within the area of study are expected to be engaging in car-following behavior before and/or after the monitored segment. Future studies will be conducted on longer arterial segments to evaluate leader-follower interactions through longer periods. Future work will also assess and quantify the improvements that can be obtained in microscopic simulation by using the proposed model to calibrate site-specific driving behavior and utilizing that as an external driver model. The end-to-end nature of this study starting with extracting vehicle trajectories from roadside cameras, and utilizing those trajectories for calibrating a data-driven driver behavior model provides a blueprint for practitioners to both accurately assess real-time traffic safety and performance, as well as aid in developing simulation models that better mimic the behavior of existing on-site traffic, allowing for a more accurate assessment of any proposed safety interventions.

REFERENCES

[1] D. C. Gazis, R. Herman, and R. B. Potts, "Car-following theory of steady-state traffic flow," *Oper. Res.*, vol. 7, no. 4, pp. 499–505, 1959.

[2] M. Bando, K. Hasebe, A. Nakayama, A. Shibata, and Y. Sugiyama, "Dynamical model of traffic congestion and numerical simulation," *Phys. Rev. E, Stat. Phys. Plasmas Fluids Relat. Interdiscip. Top.*, vol. 51, no. 2, p. 1035, 1995.

[3] M. Brackstone and M. McDonald, "Car-following: A historical review," *Transp. Res. F Traffic Psychol. Behav.*, vol. 2, no. 4, pp. 181–196, 1999.

[4] V. Punzo, M. T. Borzacchiello, and B. Ciuffo, "On the assessment of vehicle trajectory data accuracy and application to the next generation simulation (NGSIM) program data," *Transp. Res. C Emerg. Technol.*, vol. 19, no. 6, pp. 1243–1262, 2011.

[5] S. H. Hamdar, L. Qin, and A. Talebpour, "Weather and road geometry impact on longitudinal driving behavior: Exploratory analysis using an empirically supported acceleration modeling framework," *Transp. Res. C Emerg. Technol.*, vol. 67, pp. 193–213, Jun. 2016.

[6] G. S. Aoude, V. R. Desaraju, L. H. Stephens, and J. P. How, "Driver behavior classification at intersections and validation on large naturalistic data set," *IEEE Trans. Intell. Transp. Syst.*, vol. 13, no. 2, pp. 724–736, Jun. 2012.

[7] L. Chong, M. M. Abbas, A. M. Flintsch, and B. Higgs, "A rule-based neural network approach to model driver naturalistic behavior in traffic," *Transp. Res. C Emerg. Technol.*, vol. 32, pp. 207–223, Jul. 2013.

[8] P. St-Aubin, N. Saunier, L. F. Miranda-Moreno, and K. Ismail, "Use of computer vision data for detailed driver behavior analysis and trajectory interpretation at roundabouts," *Transp. Res. Record*, vol. 2389, no. 1, pp. 65–77, 2013.

[9] A. Talebpour, H. S. Mahmassani, and F. E. Bustamante, "Modeling driver behavior in a connected environment: Integrated microscopic simulation of traffic and mobile wireless Telecommun. Syst.," *Transp. Res. Res. C Emerg. Technol.*, vol. 2560, no. 1, pp. 75–86, 2016.

[10] M. Zhu, X. Wang, A. Tarko, and S. Fang, "Modeling car-following behavior on urban expressways in shanghai: A naturalistic driving study," *Transp. Res. C Emerg. Technol.*, vol. 93, pp. 425–445, Aug. 2018.

[11] H. Wang, Y. Li, W. Wang, M. Fu, and R. Huang, "Optimal velocity model with dual boundary optimal velocity function," *Transportmetrica B Transp. Dyn.*, vol. 5, no. 2, pp. 211–227, 2017.

[12] S. Mammari, S. Mammari, and H. Haj-Salem, "A modified optimal velocity model for vehicle following," *IFAC Proc. Vol.*, vol. 38, no. 1, pp. 120–125, 2005.

[13] H. Lazar, K. Rhoulemi, and M. D. Rahmani, "A modified full velocity difference model based on time to collision as a safely indicator for braking state," in *Proc. 2nd World Symp. Web Appl. Netw. (WSWAN)*, 2015, pp. 1–6.

[14] H. Lazar, K. Rhoulemi, and D. Rahmani, "A review analysis of optimal velocity models," *Periodica Polytechnica Transp. Eng.*, vol. 44, no. 2, pp. 123–131, 2016.

[15] S. Ossen and S. P. Hoogendoorn, "Car-following behavior analysis from microscopic trajectory data," *Transp. Res. Res. C Emerg. Technol.*, vol. 1934, no. 1, pp. 13–21, 2005.

[16] J. Morton, T. A. Wheeler, and M. J. Kochenderfer, "Analysis of recurrent neural networks for probabilistic modeling of driver behavior," *IEEE Trans. Intell. Transp. Syst.*, vol. 18, no. 5, pp. 1289–1298, May 2017.

[17] T. A. Wheeler, P. Robbel, and M. J. Kochenderfer, "Analysis of microscopic behavior models for probabilistic modeling of driver behavior," in *Proc. IEEE 19th Int. Conf. Intell. Transp. Syst. (ITSC)*, 2016, pp. 1604–1609.

[18] V. Papanthanasopoulou and C. Antoniou, "Towards data-driven car-following models," *Transp. Res. C Emerg. Technol.*, vol. 55, pp. 496–509, Jun. 2015.

[19] Y. Yu, "Revisit of microscopic car following models: Conventional and machine learning perspectives," Ph.D. dissertation, Faculty Eng. Inf. Technol., Univ. Technol. Sydney, Ultimo, NSW, Australia, 2021.

[20] V. G. Kovvali, V. Alexiadis, L. Zhang, "Video-based vehicle trajectory data collection," Cambridge Systematics, Inc., Oakland, CA, USA, Rep. 07-0528, 2007.

[21] V. Punzo, D. J. Formisano, and V. Torrieri, "Nonstationary Kalman filter for estimation of accurate and consistent car-following data," *Transp. Res. Res. C Emerg. Technol.*, vol. 1934, no. 1, pp. 2–12, 2005.

[22] Y. Wan, Y. Huang, and B. Buckles, "Camera calibration and vehicle tracking: Highway traffic video analytics," *Transp. Res. C Emerg. Technol.*, vol. 44, pp. 202–213, Jul. 2014.

[23] G. Guido, A. Vitale, and V. Gallelli, "Investigating rear-end potential conflicts for roundabout turning movements," *Modern Traffic Transp. Eng. Res.*, vol. 2, no. 4, pp. 20–26, 2013.

[24] P. St-Aubin, L. Miranda-Moreno, and N. Saunier, "An automated surrogate safety analysis at protected highway ramps using cross-sectional and before-after video data," *Transp. Res. C Emerg. Technol.*, vol. 36, pp. 284–295, Nov. 2013.

[25] P. St-Aubin, N. Saunier, and L. F. Miranda-Moreno, "Comparison of various time-to-collision prediction and aggregation methods for surrogate safety analysis," Transportation Research Board, Washington, DC, USA, Rep. 15-4629, 2015.

[26] P. St-Aubin, N. Saunier, and L. F. Miranda-Moreno, "Large-scale automated proactive road safety analysis using video data," *Transp. Res. C Emerg. Technol.*, vol. 58, pp. 363–379, Sep. 2015.

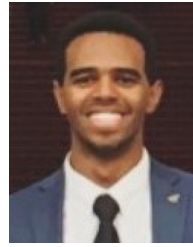
[27] K. Xie et al., "Development of a comprehensive framework for video-based safety assessment," in *Proc. IEEE 19th Int. Conf. Intell. Transp. Syst. (ITSC)*, 2016, pp. 2638–2643.

[28] K. Xie, K. Ozbay, H. Yang, and C. Li, "Mining automatically extracted vehicle trajectory data for proactive safety analytics," *Transp. Res. C Emerg. Technol.*, vol. 106, pp. 61–72, Sep. 2019.

[29] S. Das and A. K. Maurya, "Defining time-to-collision thresholds by the type of lead vehicle in non-lane-based traffic environments," *IEEE Trans. Intell. Transp. Syst.*, vol. 21, no. 12, pp. 4972–4982, Dec. 2019.

[30] M. Kilicarslan and J. Y. Zheng, "Predict vehicle collision by TTC from motion using a single video camera," *IEEE Trans. Intell. Transp. Syst.*, vol. 20, no. 2, pp. 522–533, Feb. 2019.

- [31] C. Wang, C. Xu, and Y. Dai, "A crash prediction method based on bivariate extreme value theory and video-based vehicle trajectory data," *Accident Anal. Prevent.*, vol. 123, pp. 365–373, Feb. 2019.
- [32] L. Li, R. Jiang, Z. He, X. M. Chen, and X. Zhou, "Trajectory data-based traffic flow studies: A revisit," *Transp. Res. C Emerg. Technol.*, vol. 114, pp. 225–240, May 2020.
- [33] A. Bochkovskiy, C.-Y. Wang, and H.-Y. M. Liao, "YOLOv4: Optimal speed and accuracy of object detection," 2020, *arXiv:2004.10934*.
- [34] N. Wojke, A. Bewley, and D. Paulus, "Simple online and realtime tracking with a deep association metric," in *Proc. IEEE Int. Conf. Image Process. (ICIP)*, 2017, pp. 3645–3649.
- [35] A. Abdelhalim and M. Abbas, "VT-Lane: An exploratory study of an ad-hoc framework for real-time intersection turn count and trajectory reconstruction using nema phases-based virtual traffic lanes," in *Proc. IEEE 23rd Int. Conf. Intell. Transp. Syst. (ITSC)*, 2020, pp. 1–6.
- [36] A. Abdelhalim and M. Abbas, "Towards real-time traffic movement count and trajectory reconstruction using virtual traffic lanes," in *Proc. IEEE/CVF Conf. Comput. Vis. Pattern Recognit. Workshops*, 2020, pp. 592–593.
- [37] A. Abdelhalim, M. Abbas, B. B. Kotha, and A. Wicks, "A framework for real-time traffic trajectory tracking, speed estimation, and driver behavior calibration at urban intersections using virtual traffic lanes," 2021, *arXiv:2106.09932*.
- [38] L. Wen *et al.*, "UA-DETRAC: A new benchmark and protocol for multi-object detection and tracking," *Comput. Vis. Image Understand.*, vol. 193, Apr. 2020, Art. no. 102907.
- [39] X. Hou, Y. Wang, and L.-P. Chau, "Vehicle tracking using deep sort with low confidence track filtering," in *Proc. 16th IEEE Int. Conf. Adv. Video Signal Based Surveillance (AVSS)*, 2019, pp. 1–6.
- [40] *Traffic Signal Timing Manual*. Washington, DC, USA: Federal Highway Admin., 2008.



AWAD ABDELHALIM received the B.Sc. degree in civil engineering from the University of Khartoum, Sudan, in 2014. He is currently pursuing the Ph.D. degree with The Charles E. Via, Jr. Department of Civil and Environmental Engineering, Virginia Tech.

He serves as an Instructor of Record with the College of Engineering, Virginia Tech. He has industry experience working in the private sector and with the Washington D.C Department of Transportation. His research focuses on intelligent transportation systems, traffic modeling and simulation, machine learning, and applied AI.



MONTASIR ABBAS (Member, IEEE) received the B.S. degree in civil engineering from the University of Khartoum, Sudan, in 1993, the M.S. degree in civil engineering from the University of Nebraska–Lincoln, Lincoln, NE, USA, in 1998, and the Ph.D. degree in civil engineering from Purdue University, West Lafayette, IN, USA, in 2001.

He was previously with Texas Transportation Institute, and joined Virginia Polytechnic Institute and State University (Virginia Tech) in 2005. He is currently a Professor with The Charles E. Via, Jr. Department of Civil and Environmental Engineering, Virginia Tech. His research interests include traffic control, traffic flow theory, agent-based modeling and simulation, and artificial intelligence.